Regulation of an Epitope-Tagged Recombinant Rsk-1 S6 Kinase by Phorbol Ester and erk/MAP Kinase†

J. Russell Grove, Daniel J. Price, Papia Banerjee, Ashok Balasubramanyam, Mir F. Ahmad, and Joseph Avruch*

Diabetes Unit and Medical Services, Massachusetts General Hospital and the Department of Medicine, Harvard Medical School, Boston, Massachusetts 02114

Received January 11, 1993; Revised Manuscript Received April 21, 1993

ABSTRACT: Phorbol ester tumor promoters (TPA) activate the endogenous erk/MAP kinases and Rsk S6 kinases but not the p70 S6 kinase in COS cells. DNA sequences encoding the rat Rsk-1 S6 kinase (homologous to *Xenopus* rskα), modified by insertion of a peptide epitope at the polypeptide aminoterminus, were expressed transiently in COS cells. TPA stimulates the 40S and peptide kinase activity of the recombinant epitope-tagged Rsk-1, as well as the extent of Rsk-1 autophosphorylation in vitro (^{32}P-Ser ≫ ^{32}P-Thr). Indications that the conformation of the recombinant Rsk-1 polypeptide is substantially changed after activation by TPA in situ include a retarded mobility of the Rsk-1 polypeptide on SDS–PAGE and the appearance of new ^{32}P-peptides during autophosphorylation in vitro. All these features of the TPA-activated Rsk-1 S6 kinase are abolished by dephosphorylation of the kinase in vitro with Ser/Thr phosphatase-2A. TPA increases ^{32}P incorporation into recombinant Rsk-1 by 2–3-fold (^{32}P-Ser ≫ ^{32}P-Thr). Peptide mapping exhibits a single major ^{32}P-peptide in Rsk-1 isolated from unstimulated cells and 10–12 additional ^{32}P peptides after TPA treatment in situ. Phosphorylation of basal or phosphatase-2A-treated recombinant Rsk-1 in vitro with erk2/MAP kinase increases Rsk-1 40S kinase, peptide kinase, and autophosphorylating activity, retards migration of Rsk-1 polypeptides on SDS–PAGE, and generates new sites of Rsk-1 autophosphorylation in vitro. By contrast, TPA-activated Rsk-1 is not altered in these properties by phosphorylation in vitro with erk2/MAP kinase. Activation of Rsk-1 in situ with TPA diminishes by over 90% the extent of Rsk-1 phosphorylation achieved in vitro by erk2/MAP kinase, as compared to the parallel phosphorylation of a phosphatase-2A-treated Rsk-1; basal Rsk-1 is intermediate. Peptide maps of phosphatase-2A-treated Rsk-1 after phosphorylation in vitro with erk2/MAP kinase exhibit ^{32}P-peptides that comigrate with nearly all of the ^{32}P-peptides present in TPA-activated-^{32}P Rsk-1 labeled in situ, plus several ^{32}P-peptides characteristic of Rsk-1 autophosphorylation in vitro. If Rsk-1 is heat inactivated to prevent autophosphorylation during treatment with erk2/MAP kinase in vitro, a greatly simplified Rsk-1 peptide map (^{32}P-Thr > ^{32}P-Ser) is obtained that lacks not only the characteristic sites of Rsk-1 in vitro autophosphorylation but many of the ^{32}P-peptides that comigrate with ^{32}P-Rsk-1 peptides labeled in situ during TPA activation. Thus, erk/MAP kinase or enzymes with very similar specificity are likely the sole upstream activator mediating TPA stimulation of Rsk-1 kinase in COS cells and act together with Rsk-1 autophosphorylation to achieve the final Rsk-1 phosphorylation state observed in situ.

Phosphorylation of the 40S ribosomal protein S6 on multiple residues is increased at an early time during hepatic regeneration, *Xenopus* oocyte maturation, and after insulin or mitogen treatment of cultured eukaryotic cells (Gordon et al., 1982). Present evidence indicates that insulin/mitogen-stimulated S6 phosphorylation is mediated by activation of one or both of two subfamilies of Ser/Thr protein kinase, relatively specific for S6, namely the Rsk S6 kinase and the p70 S6 kinases (Erikson, 1991). Several members of both subfamilies of these insulin/mitogen-regulated S6 protein kinases have now been characterized at a molecular level. The first to be purified was a 92 kDa polypeptide isolated from *Xenopus* eggs designated S6 kinase II to indicate its order of elution on anion-exchange chromatography (Erikson & Maller, 1986). S6 kinase I, a more labile 90 kDa enzyme, was purified only recently (Erikson & Maller, 1991). Tryptic peptide sequence derived from *Xenopus* S6 kinase II was employed to isolate several *Xenopus* cDNAs, later named rsk (ribosomal S6 kinase), whose amino acid sequence predicted a novel protein kinase that encoded two complete catalytic domains, a feature unique thusfar among the Ser/Thr protein kinases (Jones et al., 1988). The more amino terminal catalytic domain is ~40% identical to those of the kinase A/kinase C families, whereas the carboxyterminal catalytic domain is most similar to that of the phosphorylase b kinase catalytic (γ) subunit. More recently, the existence of a second, structurally distinct family of insulin/mitogen-activated S6 kinase was established by the purification and subsequent molecular cloning of the p70 S6 kinase (Banerjee et al., 1990; Kozma et al., 1990). That enzyme contains a single catalytic domain, 57% identical to the aminoterminal, kinase C-like catalytic domain of *Xenopus* Rskα. Outside of the catalytic domain, the sequences of p70 and Rsk S6 kinases are not structurally related.

cDNAs homologous to *Xenopus* rskα have been cloned from chicken (rsk-ch) and mouse (rsk-mo-1) (Alcorta et al., 1989) and rat (rsk-rat-1) (Banerjee et al., 1990) sources and encode Rsk polypeptides that share over 90% identity. In addition, a second mouse rsk-like cDNA (rsk-mo-2) was isolated whose mRNA exhibits a different tissue distribution than rsk-mo-1 and whose amino acid sequence is only 85% identical to Rsk-mo-1 (Alcorta, et al., 1989). Current evidence indicates that

† Supported in part by awards from the ACS (B-6) and NIH (DK17776). J.R.G. is a Capps Scholar in Diabetes of Harvard University. A.B. is supported by a Physician Scientist Award (K12 DK01410).

* Address all correspondence to Dr. J. Avruch, Diabetes Research Labs, MGH East, Bldg. 149, 13th Street, Charlestown, MA 02129. Telephone: (617) 726-6909. Fax: (617) 726-5649.

0006-2960/93/0432-7727$04.00/0

Rsk-mo-1 and Rsk-mo-2 are homologous to *Xenopus* S6 kinase I and S6 kinase II, respectively. Thus, certain monoclonal antibodies raised to *Xenopus* Rskα are reactive with S6 kinase I but not S6 kinase II (Erikson & Maller, 1991). Polyclonal antisera raised to purified denatured *Xenopus* S6 kinase II, although not reactive with S6 kinase I (Erikson et al., 1987), did crossreact with an insulin-activated 91 kDa rabbit skeletal muscle protein kinase designated insulin-stimulated protein kinase (ISPK)-1 (Lavoinne et al., 1991). *Xenopus* S6 kinase II and ISPK-1 exhibit an indistinguishable substrate specificity, whereas subtle but clearcut differences in the substrate specificity of *Xenopus* S6 kinase I and II were evident (Erikson & Maller, 1991). Extensive peptide sequence from rabbit ISPK-1 recently obtained in P. Cohen's lab, is identical to Rsk-mo-2.[1] Thus, it is certain that ISPK-1/S6 kinase II corresponds to Rsk-mo-2 and very likely that S6 kinase I is homologous to *Xenopus* Rskα and thus to rat and mouse Rsk-1.[2]

All the mitogen-activated S6 kinases studied thusfar, i.e., the *Xenopus* Rsk-1 and Rsk-2 enzymes (Erikson & Maller, 1989) as well as the p70 S6 kinase (Price et al., 1990), are regulated in situ by Ser/Thr phosphorylation. In regard to the *Xenopus* Rsk enzymes, insulin/progesterone treatment of *Xenopus* oocytes stimulates ^{32}P incorporation into multiple Ser (especially) and Thr residues on the enzyme polypeptides, concomitant with their activation (Erikson & Maller, 1989). Phosphatase-2A treatment deactivates *Xenopus* Rsk activity concomitant with dephosphorylation (Sturgill et al., 1988). More importantly, phosphorylation in vitro of the purified *Xenopus* S6 kinase II (Sturgill et al., 1988), as well as rabbit skeletal muscle ISPK-1 (Lavoinne et al., 1991), by p42 MAP kinase results in substantial increase in S6 kinase activity of both Rsk enzymes, whether the substrate employed is the phosphatase-treated, inactivated Rsk enzyme or the untreated, active Rsk S6 kinase. This finding, together with the observations that MAP kinases corresponding to erk-2/erk-1 are the dominant Rsk-1 kinases detected in extracts from mitogen-treated cells (Ahn & Krebs, 1990; Chung et al., 1991; Barrett et al., 1992), the similar time course of mitogen-activation of MAP kinase and Rsk activity (Chung et al., 1991), and the finding that the sites on Rsk-1 phosphorylated in vitro by p42/p44 MAP kinase correspond to at least a subset of the sites phosphorylated on Rsk-1 in response to mitogens in situ (Sturgill et al., 1988; Chung et al., 1991) all argue strongly that the erk/MAP kinases are the major, perhaps sole, upstream activators of Rsk-1 kinases. Nevertheless, several observations do not readily fit with this conclusion. First, the experiments of Sturgill et al. (1988) and Lavoinne et al. (1991), which employed highly purified preparations of S6 kinase II and ISPK-1, respectively, isolated in the active form, showed that prior phosphatase treatment of S6 kinase II/ ISPK-1 did not increase the amount of S6 kinase activity generated by subsequent Rsk phosphorylation by MAP kinase, as would be expected if phosphatase were dephosphorylating sites of activating phosphorylation catalyzed in situ by MAP kinase. In addition, the peptide maps of *Xenopus* S6 kinase II phosphorylated by p42 MAP kinase in vitro appear significantly less complex than those of *Xenopus* S6 kinase II phosphorylated in progesterone-stimulated, ^{32}P-labeled oocytes (Erikson & Maller, 1989; Sturgill et al., 1988); moreover, phosphatase treatment of S6 kinase II did not appear to make available sites for phosphorylation by MAP kinase other than those seen in the untreated, active S6 kinase II. These observations could be explained if p42 MAP kinase, despite its ability to phosphorylate and activate S6 kinase II in vitro, were not the kinase responsible for mitogen activation of Rsk in situ. These discrepancies led us to examine whether the phosphorylation of Rsk-1 that occurs in situ during activation by TPA occurs at sites phosphorylated by MAP kinase in vitro, and if so, how extensively MAP kinase is likely to contribute to Rsk-1 phosphorylation during mitogen stimulation in situ.

To address these questions, we isolated DNA sequences corresponding to rat Rsk-1 (Banerjee et al., 1990) and employed transient expression of an epitope-tagged rat Rsk-1 polypeptide in COS cells. Our data indicate that the activation of the recombinant Rsk-1 by TPA is likely to be mediated entirely by erk/MAP kinase-mediated phosphorylation of the Rsk-1 polypeptide, acting in concert with Rsk-1 autophosphorylation.

EXPERIMENTAL PROCEDURES

cDNA Library Construction, Screening, and Sequencing. cDNA libraries were constructed in λgt11 at the *Eco*RI site from poly(A)$^+$ RNA selected from rat H4 hepatoma cell lines with a kit (Amersham or BRL), using either oligo(dT) or specific and random primers for first-strand synthesis. λgt11-cDNA recombinants were packaged in vitro (Gigapak, Stratagene). An oligo(dT)-primed cDNA library (1×10^6 recombinants) was screened initially under stringent conditions (30% formamide in standard hybridization buffer (Sambrook et al., 1989) at 42 °C) with a random-primed cDNA probe derived from *Xenopus* Rskα (Jones et al., 1988), a gift from R. L. Erikson. A single 1.16 kb Rsk-1 cDNA (clone no. 9) was isolated. The DNA and amino acid sequence of clone no. 9 were about 76% and 88%, respectively, identical to those of *Xenopus* Rskα, and corresponded to the majority of the carboxyterminal catalytic domain. A 745 base pair *Eco*RI–*Pst*I fragment of clone 9 subcloned in pBS (Stratagene) was used to screen a second oligo(dT)-primed H4 library under stringent conditions, and 12 positive clones were selected. Three of the longest clones were identical, and one of them, called clone no. 25, was used for further analysis. Clone no. 25 contained a 2548 bp insert that extended between bases 583 and 3131 (coordinates in the final assembled rat Rsk-1 cDNA sequence) and at its 3′-end contained a poly(A) tail preceded by a polyadenylation signal. Analysis of the overlapping sequences of clones no. 9 and no. 25 indicated that the first-strand cDNA of clone no. 9 had been primed from an intermediate stretch of 11 adenines interrupted by a single guanine. Finally, a third H4 cDNA library, made by priming with a mixture of random primers and a specific primer (from coordinates 1421–1394) for 5′-extension, was screened with a ^{32}P-labeled probe generated by polymerase chain reaction from the extreme 5′-end of clone no. 25 (spanning bases 583–804); 18 positive clones were isolated after four rounds of screening.

To determine which clone extended furthest 5′, polymerase chain reaction was performed on the λ-phage suspension of each clone, using the 5′-directed PCR primer, S6K IV, in conjunction with each of the λ DNA terminal primers. Clone no. 27 (1.4 kb), which had been specifically primed, extended 5′ to encode the ATG start codon. To construct a cDNA encoding the full-length rat Rsk-1 S6 kinase, clone no. 27

[1] P. Cohen, personal communication.

[2] Abbreviations: TPA, tetradecanoyl phorbol acetate; Rsk-1, ribosomal S6 kinase, no. 1; Rsk-2, ribosomal S6 kinase, no. 2; PCR, polymerase chain reaction; SDS–PAGE, sodium dodecyl sulfate polyacrylamide gel electrophoresis; epi, epitope; DMEM, Dulbecco's modified Eagles medium; HRP, horseradish peroxidase; DTT, dithiothreitol.

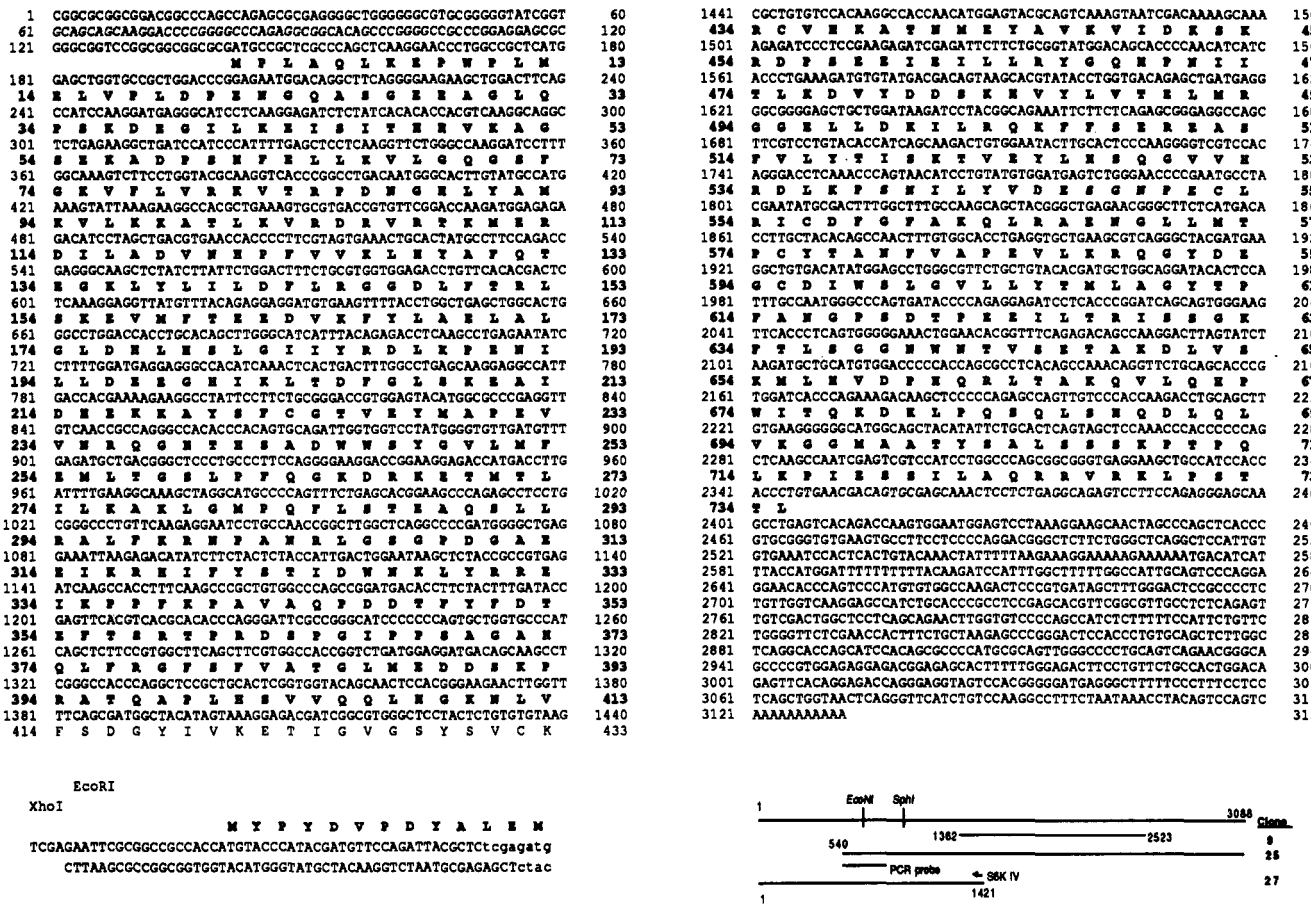

FIGURE 1: Nucleotide and protein sequence of rat Rsk-1 S6 protein kinase. Nucleotides are numbered in plain text and amino acids (indicated in single-letter code) are numbered in bold text. At the bottom is a schematic of the complete Rsk-1 sequence and maps of the cDNA clones used for its assembly.

(bases 43–1464) and clone no. 25 (bases 583–3131) were joined at the unique *Sph*I restriction site at residue 984 and introduced into the EcoRI site in the pGEM vector (pGEM-Rsk-1); the correct assembly was confirmed by restriction mapping and DNA sequencing (Figure 1).

For sequencing, the cDNA inserts isolated from λgt11-cDNA recombinants were subcloned in pBS (Stratagene) or pGEM-7Z (Promega). Sequencing was performed using the kit from United States Biochemical, employing a combination of universal sequencing primers and specific Rsk-1 primers where pertinent for some clones and using as templates a series of unidirectional nested deletions (Erase-a-Base, Promega). All sequences were determined at least twice in each strand. The University of Wisconsin Genetics Computer Group software package was used for sequence assembly, analysis, and manipulation.

In Vitro Transcription and Translation. The plasmid pGEM-Rsk-1 was linearized by digestion at a unique *Nco*I restriction site in the 3′-untranslated region, and RNA was transcribed with T7 RNA polymerase (Stratagene). Translation of 1 μg of (DNA-free) RNA was performed in rabbit reticulocyte lysates in the presence of [^{35}S]Met for 60 min at 30 °C as recommended by the supplier (Promega). The translation products were separated by SDS–PAGE and examined by fluorography.

Construction of Epitope-Tagged Rsk-1 S6 Kinase. Rat Rsk-1 cDNA was used for mammalian expression studies after subcloning into the *Eco*RI site of the mammalian expression vector pMT2 (Kaufmann et al., 1989). Introduction of the epitope (Field et al., 1988) employed PCR to introduce a *Xho*I site immediately adjacent to the initiator ATG of the rat Rsk-1 cDNA A pair of synthetic oligonucleotides was annealed and ligated into this *Xho*I site, generating pGEM-Rsk-1-epi. The oligonucleotides, whose sequences were top strand, 5′ TCGA GAA TTC GCG GCC GCC ACC ATG TAC CCA TAC GAT GTT CCA GATTAC GCT 3′, and bottom strand, 5′ TCGAG AGC GTA ATC TGG AAC ATC GTA TGG GTA CAT GGT GGG GGC CGC GAA TTC 3′, encode, in the following order, *Xho*I, *Not*I, and *Eco*RI restriction sites, a consensus translational initiation sequence CCACC, an initiator ATG, and sequences encoding a nine amino acid epitope, YPYDVPDYA. The epitope-tagged amino-terminal coding region was transferred to pMT2-Rsk-1 as an *Eco*RI-*Nde*I fragment, generating pMT2-Rsk-1-epi, which was employed in the expression studies described herein.

Eukaryotic Expression. pMT2-Rsk-1 plasmid DNA (20–25 μg per 100-mm dish) was introduced into COS-7 cells by DEAE-dextran-mediated transfection (Sambrook et al., 1989). Cells were routinely maintained in Dulbecco's modified Eagle's medium (DMEM) with 10% fetal calf serum. On the day of experiments, the medium was changed to DMEM with 0.5% serum; for ^{32}P-labeling, phosphate-free DMEM with 0.5% fetal calf serum containing 0.25–0.5 mCi/mL carrier-free $^{32}P_i$ was employed. After 3 h in 0.5% serum, TPA (0.1 μM) or carrier was added, and cells were harvested 15 min later by aspiration of medium, rapid rinsing in ice-cold phosphate-buffered saline, and extraction into homogenization buffer (10 mM potassium phosphate, pH 7.3, 10 mM $MgCl_2$, 50 mM β-glycerophosphate, 5 mM EGTA, 1 mM EDTA, 2 mM DTT, 1 mM sodium vanadate, 0.2% (w/v) Triton X-100, 2 μM pepstatin, 10 000 kallikrein inhibitor units/mL of apro-

tinin, 0.2 mM phenymethylsulfonyl fluoride, and 2 μM leupeptin). Extracts were clarified by centrifugation (100 000 × g, 45 min) and matched for protein.

Immunoblotting and Immunoprecipitation. For immunoblotting, proteins were transferred to poly(vinyl fluoride) membranes (Millipore) after SDS–PAGE. The membrane was blocked with 5% dried milk in buffered saline (20 mM Tris–HCl, pH 7.4, 150 mM NaCl) containing 0.5% Tween-20 for 1 h and incubated for 1 h with the primary antibody in the blocking buffer. After removal of the unbound antibody, the membrane was incubated for 60 min with horseradish peroxidase (HRP)-conjugated antiimmunoglobulin and washed in blocking buffer and then in buffered saline. The immunoblottable proteins were visualized by enhanced chemiluminescence (ECL, Amersham).

An antiserum directed against recombinant *Xenopus* Rskα (serum no. 125, a generous gift of R. L. Erikson) was used at a 1:500 dilution to probe for the rat Rsk-1 protein. Detection was with HRP-conjugated donkey antirabbit immunoglobin at a 1:10 000 dilution. For immunoblotting the epitope-conjugated Rsk-1, mouse monoclonal antibody 12CA5 (Niman et al., 1983) was used at a 1:10 to 1:20 dilution of the supernatant of the cultured hybridoma; detection was accomplished with HRP-conjugated sheep antimouse immunoglobin at a 1:5000 dilution.

Immunoprecipitations were performed by incubating cell extract, matched for protein, with 12CA5 antibody (1:5 dilution of the hybridoma supernatant) and protein A-agarose or protein G-Sepharose beads (1:10 dilution of a 50% suspension in homogenization buffer) on a rotating wheel at 4 °C for 3 h. The agarose beads were pelleted by low-speed centrifugation, washed extensively in homogenization buffer, in buffer A (10 mM potassium phosphate, pH 7.3, 50 mM β-glycerophosphate, 5 mM EGTA, 1 mM EDTA, 2 mM DTT, 1 mM sodium vanadate, 1% (w/v) NP-40, 0.1 M NaCl, 10% (w/v) glycerol, and 0.2 mM phenylmethylsulfonyl fluoride) or as indicated below, and used as a 50% suspension for subsequent manipulations. In some experiments Rsk-1-epi was immunoprecipitated with 12CA5 covalently coupled to agarose beads (capacity 8–10 mg of protein/mL packed bead volume) prepared as follows: Protein was precipitated from the 12CA5 hybridoma supernatant with 50% saturated ammonium sulfate, resuspended in 10 mM Tris–HCl, pH 8.5, and dialyzed exhaustively against the same buffer. The sample was applied to a DEAE-Sephacel column and eluted with a gradient of 0 to 0.6 M NaCl in the same buffer. Conjugation of the immunoglobulin peak to Affigel 10 was carried out according to the manufacturer.

Chromatography of Extracts on MonoQ. A MonoQ anion-exchange column (HR 5/5, Pharmacia) was washed extensively and equilibrated with buffer B (10 mM β-glycerophosphate, pH 7.3, 2 mM EGTA, 1 mM EDTA, 2 mM DTT, 10% (w/v) glycerol, and 0.1% (w/v) Triton X-100). Samples of cytosolic extracts, matched for protein (about 1.5 mg), were diluted with buffer C (2 mM EGTA, 1 mM EDTA, 2 mM DTT, pH 7.3) to reduce the conductivity to that of buffer B and applied in a 10-mL volume. The column was washed with 5 mL of buffer B, and proteins were eluted with an 18-mL gradient from 0 to 0.5 M NaCl in buffer B.

Protein Kinase Assay and in Vitro Autophosphorylation. Conditions for assay of 40S ribosomal S6 protein kinase and S6 peptide activity were as described previously (Price et al., 1989). Rsk-1 immunoprecipitates were washed twice in buffer A and twice in buffer D (10 mM potassium phosphate, 50 mM β-glycerophosphate, pH 7.3, 5 mM EGTA, 1 mM EDTA, 2 mM DTT, 1 mM sodium vanadate, 10% (w/v) glycerol, and 0.1% (w/v) Triton X-100) and resuspended to a 50% suspension in buffer D. Aliquots of bead suspension (30 μL) were brought to a final volume of 60 μL containing (final concentration) the following: 10 mM MOPS, pH 7.3, 10 mM $MgCl_2$, 1 mM DTT, 100 μM [γ-^{32}P]ATP (specific activity 1500–8000 cpm/pmol), and 2 μM of a synthetic peptide corresponding to residues 1–31 of the heat-stable inhibitor of the cAMP-dependent protein kinase. Rat liver 40S ribosomal subunits when present were at 16 A_{260} units/mL, final concentration; the 32 amino acid S6 peptide (Price et al., 1989) was 25 μM. Aliquots of MonoQ fractions were assayed under similar conditions. Kinase assays were incubated at 30 °C for 15 min and terminated with the addition of SDS sample buffer. S6 peptide kinase was terminated by application to p81 paper as described previously (Price et al., 1989). Autophosphorylation was carried out under identical conditions except by omission of the protein/peptide substrate.

Treatment of Rsk-1 with Protein Phosphatase. Epitope-tagged Rsk-1 immunoprecipitates were washed and resuspended in buffer E (50 mM Tris–HCl, pH 7.3, 10 mM $MgCl_2$, 2 mM EGTA, 1 mM EDTA, 2 mM DTT, 0.1% (w/v) Triton X-100, 10% (w/v) glycerol). Purified protein phosphatase-2A (a gift of D. Brautigan) was added to 5–10 units/mL; incubation was usually carried out at 30 °C for 30 min and terminated by the addition of β-glycerophosphate to 50 mM and okadaic acid to 0.4 μM.

For treatment with recombinant tyrosine-specific phosphatase (a gift of T. Ingebritsen), Rsk-1 immunoprecipitates were washed and resuspended in buffer F (10 mM potassium phosphate, 50 mM β-glycerophosphate, 2 mM EGTA, 1 mM EDTA, 2 mM DTT, 10% (w/v) glycerol). Recombinant tyrosine phosphatase (Gaun et al., 1990) was added to about 250 units/mL; incubation was carried out at 30 °C for 30 min and terminated by chilling to 4 °C and washing.

Phosphorylation of Rsk-1 in Vitro with erk2/MAP Kinase. Washed Rsk-1 immunoprecipitates were resuspended in 0.3 mL of buffer E supplemented with ATP to 0.5 mM, and 3 units of erk2/MAP kinase partially purified as described previously (Pulverer et al., 1991) (a gift of J. Kyriakis) was added. Incubation proceeded at 30 °C for 30 min; reactions were terminated by chilling to 4 °C and washing. In most experiments, the washed immunoprecipitate was also treated with tyrosine phosphatase as above.

Peptide Mapping and Phosphoamino Acid Analysis. After SDS–PAGE ^{32}P-labeled Rsk-1 was identified by autoradiography of the frozen unfixed gel. The ^{32}P-Rsk-1 was mechanically eluted from the gel, precipitated in chloroform/methanol with added unlabeled carrier (rabbit skeletal muscle phosphorylase b, 100 μg), and subjected to complete tryptic digestion exactly as described by Price et al. (1990). Two-dimensional peptide mapping on cellulose-coated plates was carried out by electrophoresis at pH 1.9 (formic acid:acetic acid:H_2O = 25:87:888) followed by chromatography (butanol = acetic acid = pyridine = H_2O = 15:3:10:12). Xylene cyanol FF was used as marker for chromatography but exhibited little migration from the origin during electrophoresis at pH 1.9. Phosphoamino acid analysis was carried out after partial hydrolysis (6 N HCl, 110 °C, 2 h) of an aliquot of the tryptic digest by two-dimensional electrophoresis (Price et al., 1990).

RESULTS

Comparative Analysis with Other Rsk S6 Kinases. The 5′-untranslated region of the rat Rsk-1 S6 kinase is highly GC-rich and has 90% identity with the mouse rsk-1 nucleotide

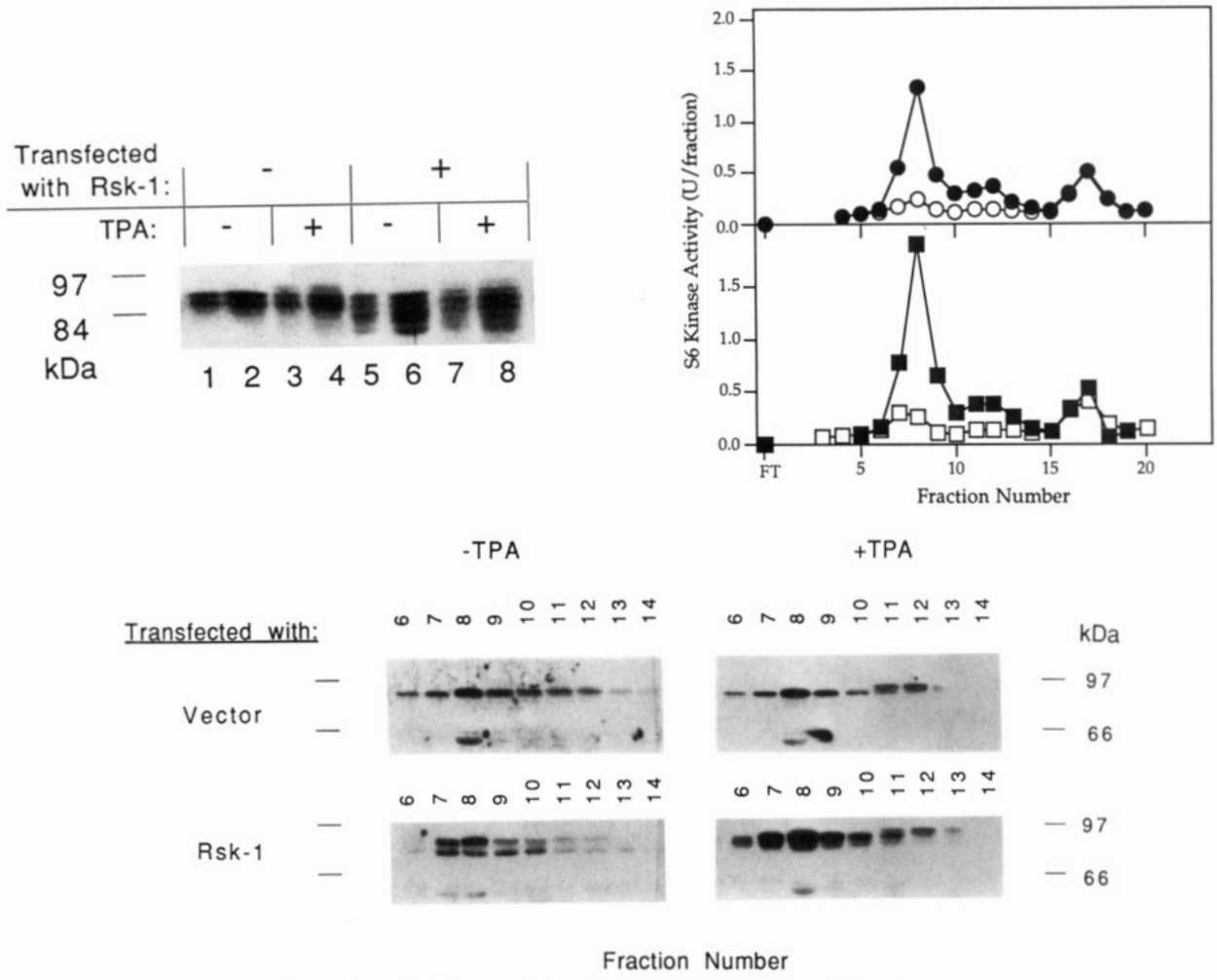

FIGURE 2: Expression of rat Rsk-1 protein and S6 kinase activity following transfection into COS cells. In A (top, left), aliquots of cytosolic protein (lanes 1, 3, 5, and 7 contain 30 μg of protein, lanes 2, 4, 6, and 8 contain 60 μg) derived from cells transfected with pMT2 alone or pMT2-Rsk-1 and treated with TPA as indicated were fractionated by SDS–PAGE, transferred to a PVDF membrane, and probed with antiserum 125, directed against recombinant *Xenopus* Rskα (Alcorta et al., 1989). In B (top, right), COS cytosolic extracts containing equal protein, obtained from cells transfected with pMT2 (circles) or pMT2-Rsk-1 (lacking the epitope tag (squares) and treated with carrier (open symbols) or TPA (0.1 μM) for 15 min, filled symbols) prior to extraction were fractionated by MonoQ anion-exchange chromatography as described in the Experimental Procedures. Fractions were assayed for S6 kinase activity (U, pmol/min) using 40S ribosomal subunits as substrate. In C (bottom), aliquots of the fractions shown in B were blotted with antiserum 125 following SDS–PAGE and transfer to PVDF.

sequence. The rat cDNA clone encodes 735 amino acids and predicts an 81.4 kDa polypeptide (Figure 1), which is 98% identical to mouse Rsk1 except that the rat sequence has an insertion of 11 amino acids (253–263aa, Figure 1) found also in *Xenopus* and chicken Rsk (Alcorta et al., 1989) but lacking in mouse. The distinguishing structural feature of the Rsk-1 subfamily of protein kinases is the presence of two protein Ser/Thr kinase catalytic domains; the more aminoterminal domain, residues 60–324, is most closely related to the single catalytic domain of the p70 family of S6 kinases (57% identity in the rat) and thereafter to the kinase C subfamily (about 40% identity). The structural similarity extends carboxy-terminal through residue 388; these additional 65 amino acid residues are approximately 40% identical between Rsk-1, p70 S6 kinase, and kinase C. The second, more carboxyterminal Rsk-1 catalytic domain (residues 416–678) is most closely related to those of the phosphorylase b kinase γ subunit (40% identity) and the Ca-calmodulin kinase II subfamily.

Expression of Endogenous S6 Kinases and Recombinant Rsk-1 S6 Kinase in COS Cells. COS cells express endogenous Rsk-like polypeptides, as indicated by immunoblot of cell extracts with antiserum 125, raised against recombinant *Xenopus* Rskα polypeptide and known to react with both *Xenopus* S6 kinase I and II (Figure 2). Transfection of COS cells with rat Rsk-1 S6 kinase cDNA sequences in the expression vector pMT2 leads to the appearance of two new immunoreactive Rsk polypeptides roughly equal in abundance to the endogenous simian Rsk polypeptides, but slightly faster in mobility on SDS–PAGE (Figure 2A). Treatment of cells with TPA shifts the ladder of endogenous and recombinant Rsk polypeptide bands to a somewhat slower R_f on SDS–PAGE.

Endogenous S6 kinase activity in COS cells is resolved into two peaks on MonoQ anion-exchange chromatography (Figure 2B). The earlier peak of S6 kinase activity overlaps with the broad peak of endogenous immunoreactive Rsk-1 polypeptides (Figure 2C), whereas the later eluting peak corresponds to p70 S6 kinase, based on anti-p70 peptide immunoblots, and coelution with recombinant p70 S6 kinase (Grove et al., 1991). Treatment of COS cells with TPA increases the S6 kinase activity in the early eluting peak by 3- to 5-fold, whereas the activity associated with p70 S6 kinase is unaffected by TPA (Figure 2B). The TPA-stimulated S6 kinase activity elutes from MonoQ as a broad and complex peak that overlaps completely the endogenous Rsk polypeptides (Figure 2C). TPA treatment results in a modest shift in the elution profile

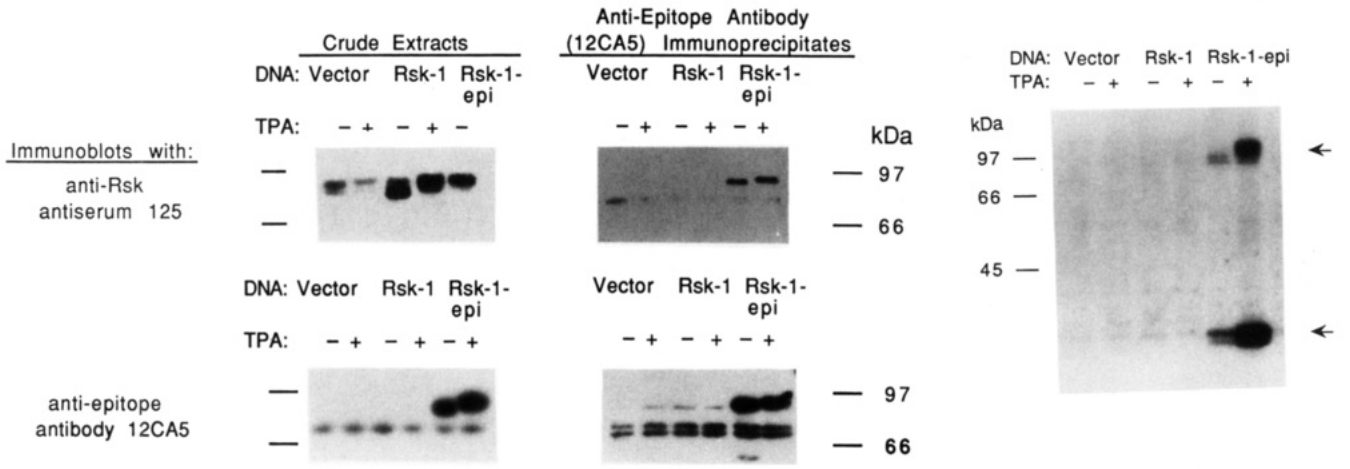

FIGURE 3: Expression of epitope-tagged rat Rsk-1 in COS cells. Cells were transfected with pMT2 containing no insert, the Rsk-1 cDNA, or Rsk-1 tagged with the epitope at the amino terminus (Rsk-1-epi), treated with carrier or TPA (0.1 μM × 15 min) and harvested. In A (left), aliquots of each extract were immunoblotted directly (left panels) or after immunoprecipitation (from 0.2 mg cytosolic protein) using the anti-epitope monoclonal antibody 12CA5 (right panels), as in the Experimental Procedures. Immunoblot employed anti-Rsk antiserum 125 (upper panels) or anti-epitope antibody 12CA5 (lower panels). In B (right), aliquots of the anti-epitope immunoprecipitates were assayed for S6 kinase activity using 40S ribosomal subunits as substrate. The upper arrow indicates the position of the Rsk-1 polypeptide; the lower arrow indicates the substrate S6.

of Rsk polypeptides toward later MonoQ fractions, as well as a retardation of the Rsk polypeptides on SDS–PAGE (Figure 2C). The ladder of endogenous polypeptides detected on SDS–PAGE after TPA treatment exhibits one or two faint bands migrating more slowly than any observed in the extract from unstimulated cells (Figure 2A,C); these slowest bands elute latest on MonoQ chromatography, coincident with a secondary peak of TPA-stimulated 40S S6 kinase activity (Figure 2B,C).

Recombinant rat Rsk-1 polypeptides, visualized by their slightly faster R_f on SDS–PAGE, are also seen to elute broadly from MonoQ, coincident with the endogenous COS Rsk polypeptides, both in the presence and absence of TPA treatment (Figure 2B). Despite the unequivocal evidence of recombinant Rsk-1 polypeptide expression, a transfection-induced increase in S6 kinase activity in either the extracts or MonoQ fractions was observed in only one of the first four transfection experiments. To determine unequivocally whether the recombinant rat Rsk-1 encoded an enzymatically active polypeptide, the Rsk-1 structure was modified by inserting, immediately after the initiator methionine, DNA sequences encoding the nonapeptide, YPYDVPDYA, followed by the authentic rat sequence. This nine-residue sequence corresponds to an epitope in the influenza hemagglutinin (HA1), reactive with the mouse monoclonal antibody 12CA5 (Wilson et al., 1984) generated by Lerner and co-workers to the influenza hemagglutinin sequence 75–110 (Niman et al., 1983).

The expression and properties of epitope-tagged Rsk-1 S6 kinase were compared to the unmodified recombinant as well as the endogenous Rsk-1 polypeptides. The epitope-tagged Rsk-1, which exhibits a slightly slower R_f on SDS–PAGE than the endogenous polypeptide (Figure 3A, upper left), is expressed at an abundance similar to that of the unmodified recombinant Rsk-1, based on immunoblot with anti-Rsk antiserum 125 (Figure 3A, upper left). Expression of the epitope-tagged Rsk-1 can also be monitored by immunoblot of COS extracts with the monoclonal anti-epitope antibody 12CA5. Several "nonspecific" endogenous bands (Figure 3A, lower panel) are seen in 12CA5 immunoblots of extracts from untransfected or vector-transfected cells; however, extracts from cells transfected with the epitope-tagged Rsk-1 exhibit a major transfection-dependent band near 97 kDa, whose R_f on SDS–PAGE is retarded slightly by TPA treatment prior to extraction. Of most importance, monoclonal antibody 12CA5 immunoprecipitates a 40S kinase activity from cells transfected with epitope-tagged Rsk1, but not from cells transfected with vector or Rsk-1-lacking epitope (Figure 3B).

TPA Activation of Recombinant Epitope-Tagged Rsk-1 in Situ. The recombinant epitope-tagged Rsk-1 polypeptides in the 12CA5 immunoprecipitate exhibit a significant basal 40S S6 kinase (Figure 4A) and S6 peptide kinase (Figure 4B) activity that is markedly stimulated by TPA treatment prior to extraction. In addition, the extent of in vitro autophosphorylation of the epitope-tagged Rsk-1 is incresed by TPA treatment prior to extraction (Figure 4C). Inasmuch as TPA does not alter the content of Rsk-1 polypeptide recovered in the 12CA5 immunoprecipitate (Figure 3A, upper right, Figure 4D), it is clear that the stimulation of 40S- and S6 peptide kinase associated with the epitope-tagged Rsk-1 polypeptide reflects an activation of Rsk-1 S6 kinase enzymatic activity. TPA treatment also induces a decrease in the mobility of the epitope-tagged Rsk-1 polypeptide on SDS–PAGE (Figure 4D), and the Rsk-1 polypeptide that exhibits the predominant increase in autophosphorylation in vitro corresponds to those exhibiting the slowest mobility on SDS–PAGE (Figures 3B, 4C), suggesting that the electrophoretically most retarded Rsk-1 polypeptides are the most catalytically active species.

Rsk-1 isolated from TPA-treated cells exhibits not only an increased extent of autophosphorylation in vitro (Figures 3C, 4C) but also on peptide mapping, an altered array of in vitro autophosphorylation sites, as compared to the enzyme isolated from basal, unstimulated cells. The peptide maps of enzyme immunoprecipitated from unstimulated cells and autophosphorylated in vitro always contain three major ^{32}P-peptides (spots 2–4; see Figures 5 and 6A–C) and the variable presence of a very basic species (spot a). The enzyme isolated from TPA-stimulated cells exhibits, in addition to spots 2–4, a very prominent spot a and numerous additional ^{32}P-peptides (e.g., b, c, e, and f, Figures 5 and 6B,D) including an array of poorly resolved ^{32}P-peptides of more acidic migration. It is likely that these new autophosphorylation sites become accessible as a result of the change in conformation that accompanies the TPA-induced activation of Rsk-1 in situ. This conformational change may also underlie the slowed mobility on

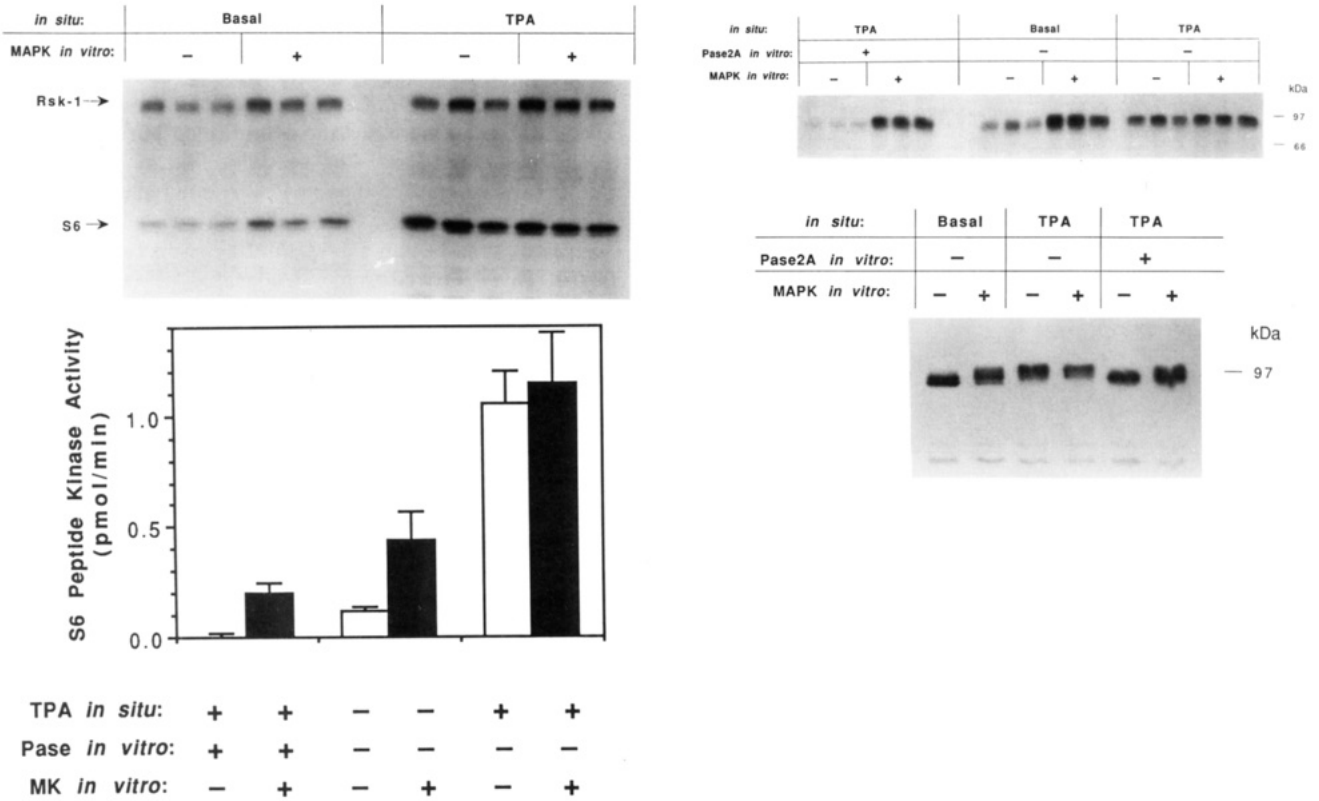

FIGURE 4: Effects of TPA in situ and MAP kinase in vitro on epitope-tagged Rsk-1. COS cells transfected with epitope-tagged Rsk-1 cDNA were treated with carrier or TPA (0.1 nM × 15 min), and Rsk-1 was immunoprecipitated with 12CA5 from aliquots of cell extracts containing equal amounts of protein. A portion of the Rsk-1 epi immunoprecipitate from TPA-treated cells was treated with the Ser/Thr-specific protein phosphastase-2A for 30 min at 30 °C, while equal aliquots of the immunoprecipitate from TPA-treated cells and a matched immunoprecipitate from the basal cells were simultaneously incubated under identical conditions but without phosphatase. The phosphatase reaction was terminated by the addition of the inhibitors okadaic acid (0.4 μM) and β-glycerophosphate (500 mM) to all samples, and phosphatase was removed by washing. All three samples were divided in half; one half was phosphorylated with MAP kinase (3 U in 0.3 mL) in the presence of 0.5 mM ATP, and the other half was incubated with ATP but without MAP kinase. The immunoprecipitates were washed to remove ATP and MAP kinase. In A (top, left) the effect of MAP kinase treatment of basal and TPA-stimulated Rsk-1 on 40S kinase activity is shown; triplicate aliquots of these extracts were assayed. The arrows indicate the migrations of Rsk-1 and of S6; this is representative of three separate experiments. In B (bottom, left) aliquots of each extract were assayed for kinase activity using the 32 amino acid S6 peptide (Price et al., 1989). The error bars indicate the standard deviation of triplicate measurements. This is representative of three separate experiments. In C (top, right) the autophosphorylation of Rsk-1 epi that occurs in the absence of substrate is shown; in this experiment, after the immunoprecipitates were washed to remove ATP and MAP kinase, they were treated with a recombinant tyrosine-specific phosphatase-1b, in order to inactivate fully any residual endogenous or added MAP kinase. This was confirmed by assay of MBP kinase following a parallel incubation with the added MAP kinase. The [γ-^{32}P]ATP was added after removal of the tyrosine phosphatase.

SDS–PAGE characteristic of the most catalytically active Rsk-1 polypeptides. Spot a in particular is a very characteristic fingerprint of the TPA-activated state, and its occasional presence in peptide maps of "basal" enzyme autophosphorylated in vitro (e.g., Figure 6C) is interpreted to reflect the abundance of "activated" Rsk-1 polypeptides in the "basal" unstimulated cells.

Dephosphorylation in vitro of the epitope-tagged Rsk-1, immunoprecipitated from basal or TPA-treated cells, with phosphatase-2A leads to deactivation of the protein kinase activity (Figure 4A,B), a diminished autophosphorylation in vitro (Figure 4C), as well as a shift of the enzyme polypeptide to a faster mobility on SDS–PAGE, as visualized by immunoblotting (Figure 4D). Okadaic acid, a specific phosphatase inhibitor, blocks the effects of phosphatase-2A (not shown). Thus, the increased Rsk-1 40S kinase activity, autophosphorylation in vitro and slowed R_f on SDS–PAGE seen after TPA treatment in situ are due to TPA stimulation of Rsk-1 Ser/Thr phosphorylation.

MAP Kinase Mediated Rsk-1 Phosphorylation in Vitro Mimics TPA Activation of Rsk-1 in Situ. TPA treatment activates an endogenous COS cell MBP/MAP kinase activity, which elutes on MonoQ chromatography in two sharp peaks that overlap the elution of erk polypeptides as detected by immunoblot (not shown). The erks are thus activated by TPA in COS cells as in many other cells and are therefore candidates for the upstream activator of Rsk-1 in these cells.

The ability of partially purified erk to activate immunoprecipitated recombinant epitope-tagged Rsk-1 in vitro is shown in Figure 4. Incubation of basal or phosphatase-2A-treated recombinant Rsk-1 with MAP kinase increases the Rsk-1 peptide/peptide kinase activity (Figure 4A,B), although not nearly to the levels seen with Rsk-1 isolated from TPA-treated cells. MAP kinase phosphorylation in vitro by MAP kinase of the Rsk-1 previously activated in situ by TPA, however, gives no further increase in Rsk-1 activity. Phosphorylation of Rsk-1 by MAP kinase in vitro also increases the extent of subsequent Rsk-1 autophosphorylation in vitro (measured after removal/inactivation of the MAP kinase) (Figure 4C) and generates a subset of Rsk-1 polypeptides that exhibit a retarded mobility on SDS–PAGE (Figure 4D).

In addition, as occurs with TPA stimulation in situ, phosphorylation of Rsk-1 in vitro with MAP kinase alters the pattern of ^{32}P-peptides generated during a subsequent in vitro Rsk-1 autophosphorylation (Figures 5 and 6C–E). Several of the MAP kinase-"generated" Rsk-1 autophosphorylation sites (spots b,c,e–g) behave similarly on peptide mapping to ^{32}P-peptides seen in digests of the Rsk-1 activated by TPA in

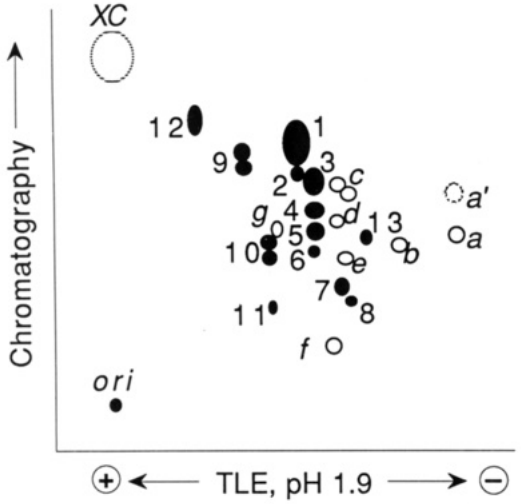

FIGURE 5: Schematic representation of 32P-Rsk-1 tryptic peptides, which enumerates the ^{32}P-peptide spots visualized in two-dimensional peptide maps of ^{32}P-Rsk-1-epi. The filled spots identified by the numbers 1–13 represent ^{32}P-peptides seen on maps of epitope-tagged ^{32}P-Rsk-1 labeled in intact COS cells; the open symbols (a–g) indicate spots seen only in maps of epitope-tagged Rsk-1 autophosphorylated in vitro in the presence of [γ-^{32}P]ATP. Certain of the numbered spots (e.g., 2–4) comigrate with spots generated during autophosphorylation in vitro. Spot a′ comigrates with spot a on TLE at pH 1.9 but is only occasionally seen in maps of Rsk-1 antiphosphorylation in vitro (e.g., as in Figure 6D,E).

situ, and subsequently autophosphorylated in vitro (Figure 6B,D).

Thus, phosphorylation of Rsk-1 by MAP kinase in vitro activates Rsk-1 catalytic functions (i.e., both protein kinase and autophosphorylation) and results in a Rsk-1 conformation that resembles that generated by TPA in situ, as reflected by the slowed R_f on SDS–PAGE, and more specifically by a similar pattern of autophosphorylation sites selected in vitro. This suggests that Rsk-1 phosphorylation by MAP kinase transforms a portion of Rsk-1 molecules to a state very similar to that of the TPA-activated state in situ.

TPA Stimulates a Multisite Phosphorylation of Rsk-1: Comparison to MAP Kinase in Vitro. TPA treatment of ^{32}P-labeled COS cells increases the overall incorporation of ^{32}P into epitope-tagged Rsk-1 by 2–3-fold (Figure 7). Tryptic peptide maps of epitope-tagged Rsk-1 isolated from basal, unstimulated ^{32}P-labeled COS cells exhibit a single major ^{32}P-peptide (spot 1) and 12–15 minor ^{32}P-peptides (Figure 8B). Enzyme prepared from TPA-treated ^{32}P-labeled COS cells (Figure 8C) exhibits substantial increases in ^{32}P incorporation into 9–10 peptides, whereas the one major ^{32}P-peptide (spot 1) and two of the minor ^{32}P-peptide (spots 7,11) observed in the basal state exhibit little or no alteration in ^{32}P content and the two ^{32}P-peptides seen in the basal state appear to decrease (spots 8, 13) (Figure 8A–C). Thus, the TPA-induced alterations in Rsk-1 catalytic activity and conformation are accompanied by increased Rsk-1 Ser/Thr phosphorylation in situ at multiple sites, and one or more of these TPA-induced Ser/Thr phosphorylations is necessary for Rsk-1 activation.

The sites on Rsk-1 phosphorylated by MAP kinase in vitro were compared to those phosphorylated during TPA stimulation in situ. Immunoprecipitated Rsk-1, treated exhaustively with phosphatase-2A in vitro, exhibits virtually no residual kinase activity (Figure 4A,B) or autophosphorylation in vitro (Figure 4C, 8G). Prolonged phosphorylation of this inactive Rsk-1 polypeptide with MAP kinase, concomitant with restoration of a portion of the Rsk-1 kinase (Figure 4B) and autophosphorylating activity (Figure 4C), leads to Rsk-1 phosphorylation at multiple sites that yield a peptide map (Figure 8F) closely resembling that of ^{32}P enzyme isolated from TPA-treated ^{32}P-labeled COS cells (Figure 8C). In fact, 12 of the 13 spots (not spot 11) detected in TPA-stimulated, in situ ^{32}P-labeled Rsk-1 are also detected in phosphatase-2A-treated Rsk-1 phosphorylated extensively by MAP kinase in vitro, and their comigration is confirmed by

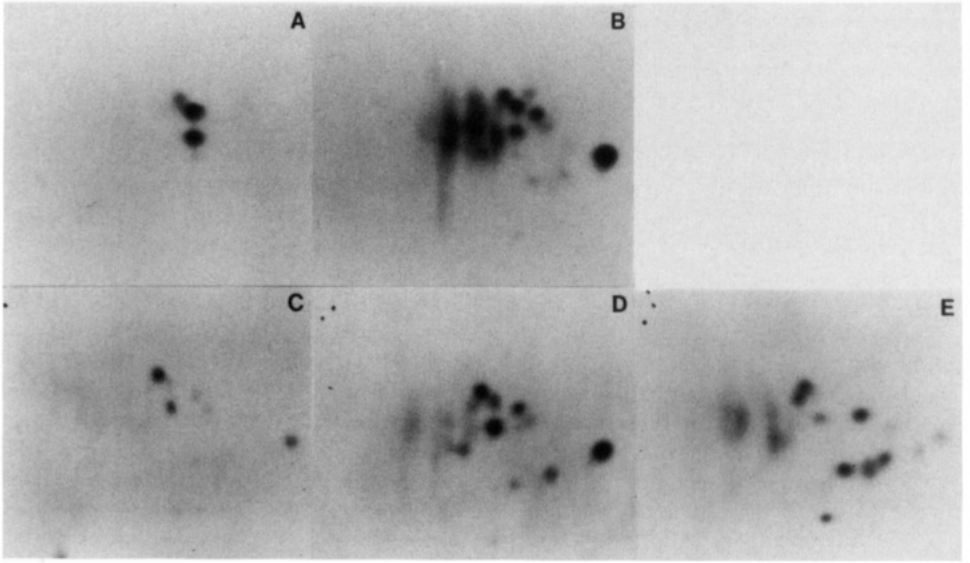

FIGURE 6: Effects of TPA in situ and MAP kinase in vitro on the site specificity of Rsk-1 in vitro autophosphorylation. COS cells transfected with epitope-tagged Rsk-1 were treated with TPA (0.1 μM) (B, D) or carrier (A, C, E) for 15 min prior to harvest. In experiment 1 (A, B), immunoprecipitated Rsk-1 was autophosphorylated in vitro with Mg (10 mM) and [γ-^{32}P]ATP for 30 min as described in the Experimental Procedures. In experiment 2 (C, D, E), the epitope-tagged Rsk-1 immunoprecipitates were incubated with recombinant tyrosine phosphatase-1b (250 U) for 30 min at 30 °C, washed in buffer D, and incubated with nonradioactive ATP (0.5 mM) at 30 °C in the absence (C, D) or presence (E) of erk2/MAP kinase (3 units). After 30 min, the immunoprecipitates were washed 2× in buffer A and 2× in buffer F and then treated with recombinant rat brain tyrosine phosphatase (250 U/mL) at 30 °C. After 30 min, the immunoprecipitates were washed once in buffer D and autophosphorylated in vitro with Mg+ [γ-^{32}P]ATP for 30 min at 30 °C as in Experimental Procedures. The reactions were terminated by addition of SDS. ^{32}P-labeled Rsk-1 was eluted from frozen SDS gels and subjected to complete tryptic digestion and two-dimensional peptide mapping as in Experimental Procedures. The autoradiographs of the plates are shown. In each panel, the origin is below the lower left corner and the xylene cyanol marker near the upper left corner, visible as dashed circles in C-E.

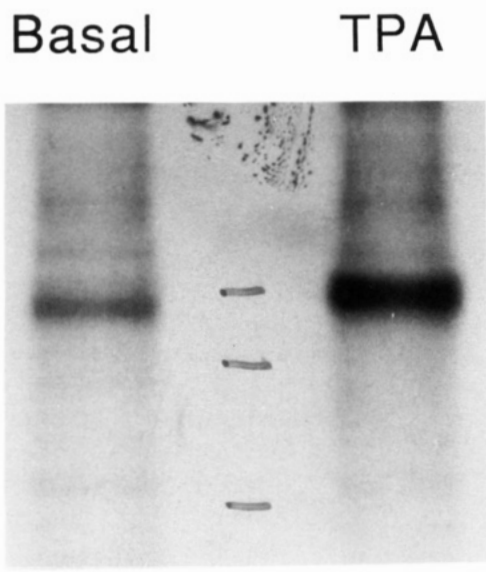

FIGURE 7: Effect of TPA on 32P incorporation into epitope-tagged Rsk-1 in COS cells. Rsk-1-epi immunoprecipitated from basal and TPA-stimulated, ^{32}P-labeled COS cells. In this experiment, COS cells were matched for protein and immunoprecipitated with 12CA5; ^{32}P content of the epitope-tagged Rsk-1 polypeptide was 14 059 cpm from basal cells and 36 324 cpm for TPA-treated cells.

mixing (Figure 8I). Three Rsk-1 ^{32}P-peptides (spots a–c) generated by phosphorylation of Rsk-1 with MAP kinase in vitro (Figure 8F) are not seen in digests of TPA-activated ^{32}P-Rsk-1 activated by TPA in situ in ^{32}P-labeled cells (Figure 8C); the most prominent is the major in vitro autophosphorylation site, spot a, characteristically seen in digests of Rsk-1 isolated from TPA-stimulated cells and autophosphorylated in vitro with [γ-^{32}P]ATP (Figure 6B,D). Conversely, several ^{32}P-peptides detected in ^{32}P-Rsk-1-labeled in situ (Figure 8B,C) are faintly (spots 8 and 13) labeled or not visualized (spot 11) after phosphorylation of Rsk-1 by MAP kinase in vitro. On balance, however, MAP kinase phosphorylation in vitro of phosphatase-2A-treated Rsk-1 generates almost all of the Rsk-1 ^{32}P-peptides that undergo phosphorylation during TPA stimulation in situ.

TPA Activation of Rsk-1 in Situ Diminishes MAP Kinase Mediated Rsk-1 Phosphorylation in Vitro. The ability of MAP kinase to catalyze ^{32}P incorporation into Rsk-1 is greatly influenced by the prior phosphorylation of Rsk-1 attained in situ (Figure 8J). Thus, Rsk-1 isolated from basal cells is much more extensively phosphorylated by MAP kinase in vitro than is the Rsk-1 isolated from TPA-stimulated cells. Phosphatase-2A treatment of Rsk-1 permits a further increment in the extent of Rsk-1 phosphorylation catalyzed by MAP kinase in vitro; these observations suggest that some of the sites on Rsk-1 undergoing phosphorylation in vitro in the presence of MAP kinase are already phosphorylated in situ in basal cells, and nearly all potential MAP kinase sites are occupied in Rsk-1 isolated from TPA-treated cells. This conclusion is strongly supported by a comparison of the ^{32}P-peptide maps of phosphatase-treated (Figure 8F), basal (Figure 8E), and TPA-activated (Figure 8D) Rsk-1 immunoprecipitated from nonradioactive cells, and phosphorylated by MAP kinase and [γ-32P]ATP in vitro, to the ^{32}P-peptide maps obtained from Rsk-1 isolated from basal (Figure 8B)

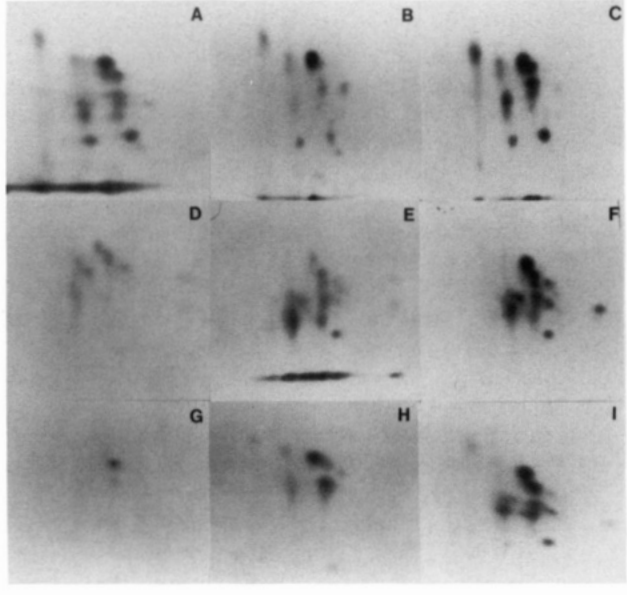

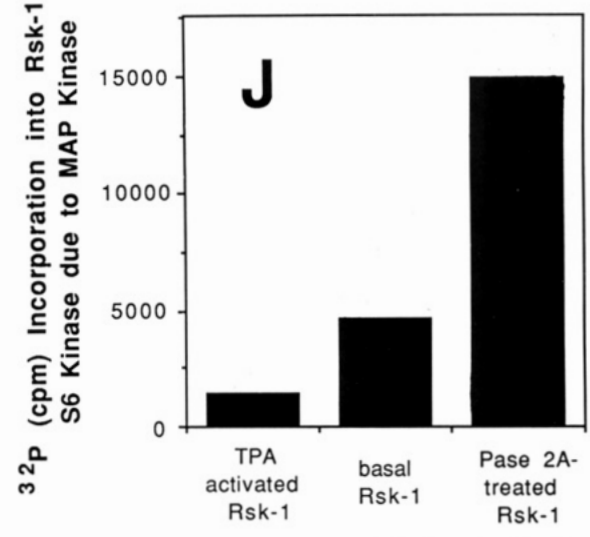

FIGURE 8: Tryptic peptide maps of ^{32}P-Rsk-1 phosphorylated in situ or in vitro with MAP kinase. Panels A–C show tryptic digests of ^{32}P-Rsk-1-epi immunoprecipitated from ^{32}P-labeled COS cells treated with TPA, 0.1 μM, for 15 min (panel C) or carrier (panel B). Approximately 1000 and 3000 cpm ^{32}P-peptide were analyzed in B and C, respectively, reflecting the ratio of overall ^{32}P incorporation into ^{32}P-Rsk-1 prior to tryptic digestion. In panel A, the digests shown individually in B and C were mixed in a 1:3 ratio of ^{32}P cpm prior to peptide separation. Panels D–F show tryptic digests of Rsk-1 immunoprecipitated from nonradioactive COS cells treated with TPA (panel D, F) or carrier (panel E) and phosphorylated with MAP kinase in vitro. The immunoprecipitate from TPA-treated cells was divided into two aliquots; one aliquot (panel F) was treated with phosphatase-2A (as in Experimental Procedures) so as to completely deactivate and extensively dephosphorylate the Rsk-1. The equal aliquots of Rsk-1 from TPA-treated cells that had (panel F) or had not (panel D) undergone phosphatase-2A treatment in vitro, as well as the matched Rsk-1 immunoprecipitate from an equal amount of extract protein prepared from unstimulated COS cells (panel E), were each phosphorylated in vitro with erk2/MAP kinase (3 U) and [γ-^{32}P]ATP. The cpm ^{32}P incorporated into each of these Rsk-1-epi substrates in the presence of MAP kinase minus the ^{32}P-cpm incorporated in the absence of MAP kinase is shown in panel J. The ^{32}P Rsk-1 polypeptides were subjected to tryptic digestion and aliquots containing ^{32}P cpm proportionate to those shown in panel J were subjected to peptide mapping. In panel G, the phosphatase-2A-treated Rsk-1 was incubated with [γ-^{32}P]ATP in the absence of MAP kinase (i.e., autophosphorylation). The exposure of panel G was approximately six times longer than those displayed in panels D–F. In panel H, an aliquot of phosphatase-2A-treated Rsk-1 was heat-inactivated (55 °C × 5 min) prior to phosphorylation with MAP kinase and [γ-^{32}P]ATP; this treatment abolished all autophosphorylation. In panel I, equal ^{32}P cpm from the Rsk-1 digests shown in panel C (TPA in situ) and panel F (MAP kinase in vitro) were mixed prior to peptide separation.

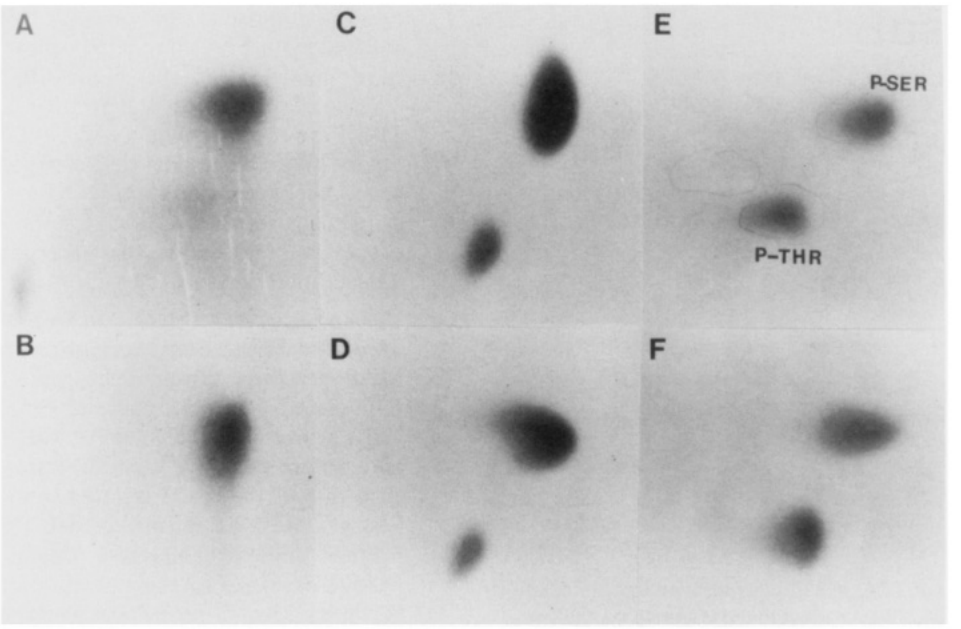

FIGURE 9: Phosphoamino acid analysis of ^{32}P-Rsk-1. The epitope-tagged ^{32}P-Rsk-1 polypeptides subjected to analysis were immunoprecipitated from the following: A, TPA-treated, ^{32}P-labeled COS cells; B, basal, ^{32}P-labeled COS cells; C, TPA-treated nonradioactive COS cells, followed by autophosphorylation in vitro with [γ-^{32}P]ATP; D, basal nonradioactive COS cells, followed by autophosphorylation in vitro with [γ-^{32}P]ATP; E, TPA-treated nonradioactive COS cells, followed by treatment with phosphatase-2A in vitro, and subsequent phosphorylation with MAP kinase and [γ-^{32}P]ATP (this treatment parallels that of the sample shown in Figure 8F); F, TPA-treated nonradioactive COS cells, followed by treatment with phosphatase-2A in vitro, and subsequent heat inactivation (55 °C × 5 min) prior to phosphorylation with MAP kinase and [γ-^{32}P]ATP (this parallels the sample in Figure 8H). The origin is at the lower left in each panel; electrophoresis was carried out toward the anode first at pH 1.9 (vertical) and then at pH 3.5 (horizontal).

and TPA-stimulated (Figure 8C) ^{32}P-labeled COS cells. MAP kinase phosphorylation of Rsk-1 isolated from basal (i.e., unstimulated) cells (Figure 8E) gives a pattern of ^{32}P spots that differs from that seen with phosphatase-2A-treated Rsk-1 (Figure 8F) in one major respect: spot 1, the major site of Rsk-1 phosphorylation in situ in unstimulated cells (Figure 8B), undergoes much less phosphorylation by MAP kinase in vitro when the substrate is Rsk-1 isolated from basal cells (Figure 8E) as compared to phosphatase-2A-treated Rsk-1 (Figure 8F), where spot 1 is the most prominent ^{32}P-peptide detected after incubation with MAP kinase and [γ-^{32}P]ATP/Mg. Thus, spot 1 is phosphorylated in basal cells and not further phosphorylated by TPA treatment in situ or MAP kinase in vitro, unless the Rsk is treated with phosphatase-2A in vitro, and then spot 1 becomes a major target for MAP kinase phosphorylation in vitro.

In contrast to the differential phosphorylation of Rsk-1 spot 1 by MAP kinase in vitro comparing basal versus phosphatase-2A-treated using these two Rsk-1 substrates, spots 2–12 are phosphorylated by MAP kinase in vitro to a comparable extent using either phosphatase-2A-treated Rsk-1 or basal Rsk-1 as substrate. The phosphorylation of spots 2–12 is greatly attenuated, however, when Rsk-1 isolated from TPA-treated cells is employed as the substrate for phosphorylation by MAP kinase in vitro (Figure 8D). TPA-activated Rsk-1 exhibits the lowest extent of overall phosphate incorporation in the presence of MAP kinase in vitro (Figure 8J), and on peptide mapping, it is evident that ^{32}P incorporation into spots 2–12 is especially diminished as compared to basal or phosphatase-2A-treated Rsk-1. Inasmuch as these spots account for most of the increase in ^{32}P content in situ after TPA treatment, the unavailability of these sites to MAP kinase in Rsk-1 isolated from TPA treated cells, together with their appearance in the peptide maps of the phosphatase 2A-treated Rsk-1 phosphorylated in vitro with MAP kinase, provides strong evidence that MAP kinase can recapitulate the phosphorylation of the specific sites of TPA-stimulated phosphorylation on 9 of the 10 ^{32}P-tryptic peptide spots whose ^{32}P content is increased after TPA treatment in situ.

Rsk Autophosphorylation Contributes to MAP Kinase-Mediated Rsk Phosphorylation. erk/MAP kinase exhibits a novel proline-directed substrate specificity such that a proline residue is required immediately carboxyterminal to the Ser/Thr phosphorylation site (Erikson et al., 1990; Alvarez et al., 1991; Mukhopadhyay et al., 1992). The rat Rsk-1 polypeptide contains six such Ser/Thr-Pro doublets that include five threonine (amino acid residues 359, 583, 612, 621, 711) and one serine (363) located on five potential tryptic peptides (Figure 1). Partial acid hydrolysis of ^{32}P-Rsk-1 immunoprecipitated from ^{32}P-labeled COS cells shows primarily ^{32}P-Ser and a small amount of ^{32}P-Thr. The TPA-induced increment is predominantly recovered in ^{32}P-Ser; nevertheless, TPA treatment does increase slightly the fractional content of ^{32}P-Thr (Figure 9A,D). The very large number of Rsk-1 tryptic ^{32}P-peptides generated in response to TPA in situ, and the fact that the predominant ^{32}P-phosphoamino acid recovered from ^{32}P Rsk-1 isolated from TPA-treated cells is ^{32}P-Ser (Figure 9A), led us to question whether MAP kinase itself catalyzed directly phosphorylation of all of the 12–14 ^{32}P-peptides detected in Rsk-1 after TPA stimulation in situ (Figure 8C) or after Rsk-1 phosphorylation by MAP kinase in vitro (Figure 8F). If prior to phosphorylation in vitro by MAP kinase, the phosphatase-2A-treated Rsk-1 is subjected to a brief heat inactivation (55 °C × 5 min) sufficient to eliminate autophosphorylation, the pattern Rsk-1 site-specific phosphorylation generated by MAP kinase is greatly simplified (compare Figure 8H to F), with spot 1 and spot 3 predominating and minor contributions from spot 7, and perhaps spots 9 and 12. In this circumstance, ^{32}P-Thr is recovered in slight excess over ^{32}P-Ser (Figure 9F). Omission of the heat inactivation steps, in addition to resulting in many more ^{32}P-peptides (Figure 8F), generates nearly equal amounts of ^{32}P-

Ser and ^{32}P-Thr (Figure 9E). Autophosphorylation of basal and TPA-stimulated Rsk-1 in vitro generates 5–10-fold more ^{32}P-Ser than ^{32}P-Thr (Figure 9C,D). On the basis of these observations, we infer that the ^{32}P-peptide maps generated from Rsk-1 isolated from TPA-treated ^{32}P-labeled COS cells reflects the combined effects of direct phosphorylation by MAP kinase (^{32}P-Thr $\geq$ ^{32}P-Ser) and Rsk-1 autophosphorylation (^{32}P-Ser $\gg$ ^{32}P-Thr), with autophosphorylation accounting for the majority of total ^{32}P incorporation into Rsk-1.

DISCUSSION

In the present study, addition of an epitope tag has enabled the characterization of the recombinant Rsk-1 enzyme activity after transient expression in a mammalian cell, in response to the extracellular regulator TPA and in comparison to the endogenous Rsk isoforms. The choice of TPA as the extracellular agonist to induce Rsk activation was arbitrary. Epitope-tagged Rsk-1 as well as the endogenous Rsk and the erk1 and 2 MAP kinases in COS cells are also activated by EGF (Price et al., 1992). We presume TPA action is mediated by kinase C, although the site of action of kinase C in the signal tranduction cascade leading to Rsk activation has not been explored in this study. Kinase C, however, is unable to activate *Xenopus* S6 kinase II directly in vitro (Sturgill et al., 1988). In view of the ability of MAP kinase, acting in vitro, to recapitulate nearly all the changes in epitope-tagged Rsk-1 wrought by treatment with TPA in situ, and the ability of TPA to activate erk in COS cells, it is likely that in these cells kinase C acts predominantly upstream of erk, perhaps at the level of ras (Wood et al., 1992; de Vries-Smits et al., 1992).

In response to TPA, five distinguishable alterations can be detected in the recombinant Rsk-1: (1) an increase of 40S and peptide kinase activity; (2) an increase in the extent of autophosphorylation in vitro; (3) the appearance of new sites of in vitro autophosphorylation, not seen with the basal, unstimulated enzyme, (4) retarded mobility of a subset of molecules on SDS–PAGE, and (5) an increase in ^{32}P-Ser (especially) and ^{32}P-Thr content distributed on >10 tryptic ^{32}P-peptides. Each of these TPA-induced changes can be reversed by treatment of the recombinant rsk by protein phosphatase-2A in vitro. The delineation of these alterations in Rsk-1 in response to TPA has enabled a detailed inquiry as to the role of MAP kinase as the proximate agent of TPA action on Rsk-1. The results indicate that phosphorylation of Rsk-1 in vitro with MAP kinase can recapitulate nearly all of the modifications observed with TPA treatment in situ.

Although several studies have demonstrated MAP kinase phosphorylation of Rsk-1 isoforms in vitro, the present results are the first to show that Rsk-1 can be activated by phosphorylation in vitro with MAP kinase. If the Rsk-1 activity attained after TPA treatment in situ is arbitrarily considered 100%, then Rsk-1 isolated from basal cells exhibits an activity that varies from 7.5% up to 20%; the activity of basal Rsk is increased to 30–40% by phosphorylation in vitro with MAP kinase. Conversely, MAP kinase phosphorylation in vitro of Rsk-1 isolated from TPA-treated cells increases Rsk-1 activity to 105%, an increment that is not significantly greater than the initial activity. These increments in Rsk-1 activity correlate with the relative extent of MAP kinase mediated ^{32}P incorporation in vitro into these two Rsk-1 substrates; the basal Rsk-1 exhibits much more ^{32}P incorporation than the Rsk-1 from TPA-stimulated cells (Figure 8J). The quantitative relationship between Rsk-1 phosphorylation by MAP kinase in vitro and the acquisition of kinase activity is not linear, however, as illustrated by the response of the phosphatase-2A-treated Rsk-1. This substrate exhibits a greater extent of ^{32}P incorporation in the presence of MAP kinase than is seen with the basal unstimulated Rsk-1; however, the increment in Rsk-1 activity from 0 to 10–15% of the TPA-stimulated Rsk-1 is considerably less than the increment in activity observed after MAP kinase phosphorylation of the basal enzyme. This response could simply reflect mild denaturation of the Rsk-1 engendered by the phosphatase treatment. Nevertheless, the nonlinear relationship between Rsk-1 phosphorylation and catalytic activity is consistent with the behavior reported earlier for the baculoviral recombinant *Xenopus* Rsk-1 coexpressed with active v-src (Vik et al., 1989). Those results suggested that only the most extensively phosphorylated Rsk-1 polypeptides, exhibiting the slowest R_f on SDS–PAGE, acquired 40S kinase activity. It appears that recombinant Rsk-1 isolated from basal, unstimulated COS cells consists of polypeptides that are partially phosphorylated (i.e., predominantly on spot 1) but not yet active, admixed with a small fraction of highly phosphorylated Rsk-1 polypeptides that are catalytically active toward 40S subunits. TPA treatment increases overall Rsk-1 ^{32}P content in situ by 2–3-fold over basal levels whereas the 40S kinase activity increases 5–15-fold. Phosphatase treatment dephosphorylates not only the active Rsk polypeptides but also the partially phosphorylated but not yet catalytically active population. On subsequent phosphorylation in vitro of the phosphatase-treated Rsk1 with MAP kinase, phosphorylation that restores phosphate to the "basal" sites will probably not be reflected by an increase in 40S kinase activity.

In addition to the activation of Rsk 40S kinase, MAP kinase-mediated phosphorylation of Rsk-1 in vitro also resulted in increased Rsk-1 autophosphorylation and, more importantly, the appearance of new Rsk-1 autophosphorylation sites. It is important to emphasize that this result is not due simply to phosphorylation catalyzed by MAP kinase carried over from the first incubation because, in addition to washing the immune complex between reactions, the complex was treated with a recombinant tyrosine phosphatase in an amount sufficient to deactivate fully any added MAP kinase. Moreover, the Rsk-1 in vitro autophosphorylation sites are ^{32}P-Ser residues almost exclusively, whereas MAP kinase-catalyzed phosphorylation of Rsk-1 exhibits a major or dominant element of ^{32}P-Thr (Figure 8F). Finally, MAP kinase does not directly phosphorylate site a (Figure 8H), a characteristic Rsk-1 autophosphorylation site in vitro. Many of the "new" Rsk-1 autophosphorylation sites generated by prephosphorylation in vitro with MAP kinase migrate very similarly on TLE/TLC to a subset of the autophosphorylation sites detected in peptide maps of Rsk-1 isolated from TPA-stimulated cells and autophosphorylated in vitro; these autophosphorylation sites are minimally represented in maps of basal Rsk-1 autophosphorylated in vitro (Figure 6A,C). In other words, MAP kinase phosphorylation of Rsk in vitro generates a set of new Rsk-1 in vitro autophosphorylation sites similar on TLE/TLC to those created by TPA treatment in situ. This provides strong evidence that MAP kinase converts a portion of the Rsk-1 polypeptides to a new conformational state which resembles closely that generated in situ in response to TPA.

The strongest evidence supporting the central role of MAP kinase in the TPA-induced activation of Rsk-1 comes from the comparisons of the ^{32}P peptide maps of Rsk-1 phosphorylated in situ and Rsk-1 phosphorylated in vitro by MAP kinase (Figure 8C,F,I). These maps contain many ^{32}P-peptides with overlapping mobility on TLC/TLE. Inasmuch as none of these peptides has been identified by direct sequence analysis,

the coidentity inferred from their comigration is not securely established. Nevertheless, MAP kinase-mediated phosphorylation in vitro of phosphatase-2A treated, totally inactive/dephospho-Rsk-1 recreates ^{32}P-peptides that comigrate with 10 of the 11 ^{32}P-peptides whose ^{32}P content is increased in the TPA-stimulated enzyme ^{32}P-labeled in situ (Figure 8I). Equally important, there is progressive loss in the availability of these sites to MAP kinase as the phosphate content of the Rsk-1 substrate increases progressively, due to phosphate incorporated in situ, ascending from the basal (Figure 8E) to the TPA-activated Rsk-1 (Figure 8D). Together, these results indicate strongly that the sites on Rsk-1 phosphorylated by MAP kinase in vitro are the same sites modified by TPA in situ and that MAP kinase is the primary and probably the sole mediator of TPA regulation of Rsk-1 in situ.

The detailed mechanism by which MAP kinase phosphorylation of Rsk-1 generates a catalytically active 40S kinase remains to be worked out. The present data indicate that the initial, "preferred" sites of MAP kinase-catalyzed Rsk-1 phosphorylation in vitro are on a limited number of residues, probably corresponding to one or more of the five threonine-proline doublets and the single serine-proline doublet preferred by MAP kinase. Paradoxically, the Rsk-1 ^{32}P-labeled in situ and isolated after TPA stimulation exhibits much more ^{32}P-Ser than ^{32}P-Thr. Inasmuch as rat Rsk-1 contains only a single serine-proline doublet, the dominance of ^{32}P-Ser on Rsk-1 after TPA treatment suggests that a majority of Rsk-1 phosphorylation during TPA activation in situ is not catalyzed directly by MAP kinase. Nevertheless the similarity of the ^{32}P-peptide maps of Rsk-1 phosphorylated extensively by MAP kinase in vitro to that seen after TPA stimulation in situ indicates strongly that MAP kinase and Rsk-1 together in vitro are sufficient to recapitulate the in situ TPA activation reaction. This apparent paradox can probably be resolved by factoring the contribution of MAP kinase-stimulated Rsk-1 *auto*phosphorylation (which is almost entirely on ^{32}P-Ser) to overall TPA-stimulated Rsk-1 phosphorylation. This plausible hypothesis leaves open several important questions: first, what are the specific residues that are modified by MAP kinase and autophosphorylation, respectively? Second, to what extent does the Rsk-1 autophosphorylation contribute to the acquisition of 40S kinase activity, or is autophosphorylation a functionally silent modification occurring simply as a passive consequence of Rsk-1 activation? These and related questions will be best answered by examining the properties of recombinant epitope-tagged Rsk-1 molecules, modified by site-directed mutagenesis.

ACKNOWLEDGMENTS

We thank Ray Erikson for the gift of *Xenopus* Rskα cDNA and anti-Rsk antiserum 125, D. Brautigan for protein phosphatase-2A, T. Ingebritsen for tyrosine phosphatase, J. Kyriakis for MAP kinase, J. Maller, P. Cohen, and J. Kyriakis for helpful discussions, Martha Chambers for preparation of the manuscript, and Carl Kozlowsky for technical assistance.

REFERENCES

Ahn, N. G., & Krebs, E. G. (1990) *J. Biol. Chem. 265*, 11495–11501.

Alcorta, D. A., Crews, C. M., Sweet, L. J., Banstron, L., Jones, S. W., & Erikson, R. L. (1989) *Mol. Cell Biol. 9*, 3850–3859.

Alvarez, E., Northwood, I. C., Gonzales, F. A., Latour, D. A., Seth, A., Abate, C., Curran, T., & Davis, R. J. (1991) *J. Biol. Chem. 266*, 15277–15285.

Banerjee, P., Ahmad, M., Grove, J. R., Kozlowsky, K., Price, D. J., & Avruch, J. (1990) *Proc. Natl. Acad. Sci. U.S.A. 87*, 84550–8554.

Barrett, C. B., Erikson, E., & Maller, J. L. (1992) *J. Biol. Chem. 267*, 4408–4415.

Chung, J., Pelech, S. L., & Blenis, J. (1991) *Proc. Natl. Acad. Sci. U.S.A. 88*, 4981–4985.

Chung, J., Chen, R.-H., & Blenis, J. (1991) *Mol. Cell Biol. 11*, 1168–1174.

de Vries-Smits, A. M. M., Burgering, B. M. T., Leevers, S. J., Marshall, C. J., & Bos, J. L. (1992) *Nature 357*, 602–604.

Erickson, A. K., Payne, D. M., Martino, P. A., Rossomando, A. J., Shabanowitz, J., Weber, M. J., Hunt, D. F., & Sturgill, T. W. (1990) *J. Biol Chem. 265*, 19728–19735.

Erikson E., & Maller, J. L. (1986) *J. Biol. Chem. 261*, 350–355.

Erikson, E., Stefanovic, D., Blenis, J., Erikson, R. L., & Maller, J. L. (1987) *Mol. Cell Biol. 7*, 3147–3155.

Erikson, E., & Maller, J. L. (1989) *J. Biol. Chem. 264*, 13711–13717.

Erikson, E., & Maller, J. L. (1991) *J. Biol. Chem. 266*, 5249–5255.

Erikson, R. L. (1991) *J. Biol. Chem. 266*, 6007–6010.

Field, J., Nikawa, J.-I., Brock, D., MacDonald, B., Rodgers, L., Wilson, I. A., Lerner, R. A., & Wigler, M. (1988) *Mol. Cell Biol. 8*, 2159–2165.

Gaun, K., Haun, R. S., Watson, S. J. Geahlin, R. L., & Dixon, J. E. (1990) *Proc. Natl. Acad. Sci. U.S.A. 87*, 1501–1505.

Gordon J, Nielsen, P. J., Manchester, K. L., Towbin, H., Jimenez de Asua, L., & Thomas, G. (1982) *Curr. Top. Cell. Reg. 21*, 89–99.

Grove, J. R., Banerjee, P., Balasubramanyam, A., Coffer, P. J., Price, D. J., Avruch, J., and Woodgett, J. R. (1991) *Mol. Cell Biol. 11*, 5541–5550.

Jones, S. W., Erikson, E., Blenis, J., Maller, J. L., & Erikson, R. L. (1988) *Proc. Natl. Acad. Sci. U.S.A. 85*, 3377–3381.

Kaufmann, R. J., Davies, M. V., Pathak, V. K., & Hershey, J. W. B. (1989) *Mol. Cell Biol. 9*, 946–958.

Kozma, S. C., Ferrari, S., Bassand, P., Siegmann, M., Totty, N., & Thomas, G. (1990) *Proc. Natl. Acad. Sci. U.S.A. 87*, 7365–7369.

Lavoinne, A., Erikson, E., Maller, J. L., Price, D. J., Avruch, J., & Cohen, P. (1991) *Eur. J. Biochem. 199*, 723–728.

Mukhopadhyay, N. K., Price, D. J., Kyriakis, J. M., Pelech, S., Sanghera, J., & Avruch, J. (1992) *J. Biol. Chem. 267*, 3325–3335.

Niman, H. L., Haughten, R. A., Walker, L. E., Reinsfeld, R. A., Wilson, I. A., Hogle, J. M., & Lerner, R. A. (1983) *Proc. Natl. Acad. Sci. U.S.A. 80*, 4949–4953.

Price, D. J., Nemenoff, R. A., & Avruch, J. (1989) *J. Biol. Chem. 264*, 13825–13833.

Price, D. J., Gunsalus, J. R., & Avruch, J. (1990) *Proc. Natl. Acad. Sci. U.S.A. 87*, 7944–7948.

Price, D. J., Grove, J. R., Calvo, V., Avruch, J., & Bierer, B. (1992) *Science 257*, 973–977.

Pulverer, B. J., Kyriakis, J. M., Avruch, J., Nikolakaki, E., & Woodgett, J. R. (1991) *Nature 353*, 670–674.

Sambrook, J., Fritsch, E. F., & Maniatis, T. (1989) *Molecular Cloning: A Laboratory Manual*, 2nd ed., Cold Spring Harbor Press, Cold Spring Harbor, NY.

Sturgill, T. W., Ray, L. B., Erikson, E., & Maller, J. L. (1988) *Nature 334*, 715–718.

Vik, T. A., Sweet, L. J., & Erikson, R. L. (1989) *Proc. Natl. Acad. Sci. U.S.A. 87*, 2685–2689.

Wilson, I. A., Niman, H. L., Haughten, R. A., Cherenson, A. R., Connolly, M. L., & Lerner, R. A. (1984) *Cell 37*, 767–778.

Wood, K. W., Sarnecki, C., Roberts, T. M., & Blenis, J. (1992) *Cell 68*, 1041–1050.